Temperature-dependent determination of electron heat capacity and electron-phonon coupling factor for $Fe_{0.72}Cr_{0.18}Ni_{0.1}$

Jan Winter,[1,*] Jürgen Sotrop,[1] Stephan Borek,[2] Heinz P. Huber,[1] and Jan Minár[2,3]

[1]*Department of Applied Sciences and Mechatronics, Munich University of Applied Sciences, Lothstrasse 34, 80335 Munich, Germany*

[2]*Department Chemie, Ludwig-Maximilian-University Munich, Butenandtstrasse 5-13, 81377 Munich, Germany*

[3]*New Technologies-Research Center, University of West Bohemia, Univerzitni 8, 306 14 Pilsen, Czech Republic*

(Received 19 June 2015; revised manuscript received 17 March 2016; published 14 April 2016)

A theoretical approach using *ab initio* calculations was applied to study the interaction of an ultrashort laser pulse with the metal alloy $Fe_{0.72}Cr_{0.18}Ni_{0.1}$ (AISI 304). The electronic structure was simulated by taking into account the chemical and magnetic disorder of the alloy by the coherent potential approximation implemented in a fully relativistic Korringa-Kohn-Rostoker formalism in the framework of spin density functional theory. A self-consistent calculation of the electronic structure using the Matsubara technique in the paramagnetic state of $Fe_{0.72}Cr_{0.18}Ni_{0.1}$ for finite temperatures was applied. Utilizing these predictions we determined the electron heat capacity and the electron-phonon coupling factor of $Fe_{0.72}Cr_{0.18}Ni_{0.1}$ in dependence on the electron temperature for two-temperature model applications. Compared with pure Fe a maximum deviation of 5% for the electron heat capacity and 25% for the electron-phonon coupling factor was found.

DOI: 10.1103/PhysRevB.93.165119

I. INTRODUCTION

Ultrashort laser pulses have a broad range of industrial applications and have been used for surface modifications of solid materials and precise micromachining [1–3]. In order to further optimize the laser process in the industrial application a deep understanding of the dynamics behind the laser ablation is essential. The theoretical description of laser-matter interaction demands a predictive modeling in irradiating a material target with an ultrashort laser pulse. Ultrafast laser irradiation of a target material induces a nonequilibrium state between the electron and lattice temperature. For metals, the nonequilibrium processes induced in a target during the energy deposition with the accessible laser fluencies can be described by the two-temperature model (TTM) [4,5]. The TTM can be written as the energy balance of two coupled nonlinear differential equations, which describe the spatial and temporal evolution of the electron and lattice temperatures:

$$C_e(T_e)\frac{\partial T_e}{\partial t} = \nabla \cdot [K_e(T_e,T_l)\nabla T_e] - G(T_e)(T_e - T_l) + S, \tag{1}$$

$$C_l(T_l)\frac{\partial T_l}{\partial t} = \nabla \cdot [K_l(T_l)\nabla T_l] + G(T_e)(T_e - T_l). \tag{2}$$

where C is the heat capacity and K is the thermal conductivity with respect to the temperature of the electron and lattice denoted by subscripts e and l, G is the electron-phonon coupling factor, and S is the laser heating source term.

The model is based on the absorption of the laser pulse energy by the valence band electrons in metals and energy transfer from the hot electrons to the lattice vibrations due to electron-phonon coupling by an energy relaxation processes. The heat diffusion from this irradiated hot surface into the bulk material of the target is described by the Fourier law. In the majority of cases, for ultrashort laser pulses the lattice heat conduction described in Eq. (2) can be neglected in comparison to the electron heat conduction in metals. Based on this, the absorption of ultrashort laser pulses by the electrons result in a transient, strong nonequilibrium of electrons and lattice due to the small heat capacity of the electron, and the long thermalization times of both electrons and lattice. The laser energy deposited in the irradiated metal target is stored in the electron subsystem while the lattice remains at a considerably low temperature. Accordingly, the electron temperature can increase by up to $\sim 10^5$ K, such that there is a temperature dependency of the thermophysical parameters of the target material included in the TTM equations. Therefore, in order to obtain accurate results in the determination of these parameters, i.e., the electron heat capacity $C_e(T_e)$, electron-phonon coupling factor $G(T_e)$ and electron thermal conductivity $K_e(T_e)$, the temperature dependence cannot be neglected when using calculation methods.

In the beginning the first models for the description of laser ablation process were based on the free electron gas. More sophisticated models took the electronic structure from *ab initio* calculation [6]. The application of these models is limited to the description of metals. We extend these theoretical considerations to include chemical and magnetic disorder into the calculation of the electronic structure using the coherent potential approximation. This is essential for the description of technical relevant alloys like stainless steel.

It is well known that for transition metals the main electronic and magnetic properties can be ascribed to the d-band electrons. For the thermophysical behavior the d band has an essential influence due to the thermal excitation of low-lying d-band electrons [7]. Therefore the d band has to be taken into account for the calculation of the electron heat capacity and the electron-phonon coupling factor. The electron temperature dependence of thermophysical parameters and the effects by thermal excitation of d-band electrons have been analyzed by Lin *et al.* [8,9]. This analysis connected the electronic structure calculations to the temperature dependence of the electron heat capacity and electron-phonon coupling factor. The results were compared with the free electron

*jan.winter@hm.edu

gas approximation and was related especially to the thermal excitation of d-band electrons. Previous work focused on detailed calculations of the electron temperature dependency of thermophysical parameters, in particular of electron heat capacity and electron-phonon coupling factor of noble and other transition metals based on the analysis of the electronic structure by Lin *et al.* [6]. Nevertheless, there is still a lack of knowledge for the basic thermophysical electronic data, especially for industrial relevant materials like metal alloys, e.g., stainless steel.

In this paper we present the electron temperature dependencies of the electron heat capacity and electron-phonon coupling factor for the commercial stainless steel alloy $Fe_{0.72}Cr_{0.18}Ni_{0.1}$ (AISI 304) in the paramagnetic face-centred cubic (fcc) crystallographic structure. The calculation of the well-known austenitic stainless steel AISI 304 is based on electronic structure calculations performed within the spin density functional theory. The structure of the paper is as follows. In Sec. II the theoretical background and computational methods used for the calculation of the electronic density of states (DOS) and for the electron heat capacity as well as the electron phonon coupling factor are described. In Sec. III our results of the thermal properties are compared with predictions for fcc-Fe. Finally we discuss the impact of the temperature on the electronic structure in the paramagnetic state of AISI 304 steel alloy. In Sec. IV a brief summary of the results is given.

II. THEORY AND METHODS

A. Electronic structure calculation

The electronic structure is obtained from *ab initio* calculations using the spin polarized relativistic Korringa-Kohn-Rostoker (SPR-KKR) band structure program package [10,11]. In this method the corresponding electronic bands of a material are calculated by solving the Dirac equation using the Green function formalism. For our calculations a fully relativistic implementation of the KKR-formalism within framework of spin density functional theory is used [11–13].

To determine the electronic structure of the austenitic stainless steel, e.g., $Fe_{0.72}Cr_{0.18}Ni_{0.1}$ it is necessary to treat the system as a disordered type of a solid state crystal. Therefore the coherent potential approximation (CPA) was applied [14]. In terms of the CPA it is possible to represent a disordered or disturbed system as a hypothetical ordered effective medium. The resulting Green function of the disordered medium can be represented as a configuration averaged Green function [15]. In that sense a system of randomly distributed disordered atoms is assumed. The calculation of the paramagnetic state above the Curie temperature was performed in a disordered local moment (DLM) model [16].

It was shown previously by Vitos *et al.* [17] that for the determination of the correct electronic structure as well as the elastic properties of the stainless steel alloy the DLM model is appropriate. In this model the two spin directions of Fe are distributed on two potentials on one lattice site representing a disordered magnetic state. It is assumed that the effective host potential is occupied by 50% electrons with spin up and 50% electrons with spin down direction, hence the configuration averaged Green function of the effective medium includes the magnetic and the chemical disorder of $Fe_{0.72}Cr_{0.18}Ni_{0.1}$. The chemical disorder was considered due to the elements included according to their stoichiometric composition. For the calculation of the effective CPA medium the Mills algorithm was used [18,19]. The exchange and correlation interaction of the electrons were described using the exchange correlation functional in the parametrization of Vosko, Wilk, and Nusair [20], i.e., the calculations were done applying the local spin density approximation (LSDA). Additionally we applied the self-consistent calculation of the electronic structure for finite temperatures. As it has been shown finite temperatures can be treated in the framework of a Green function method considering the Fermi-Dirac distribution [21]. Therefore one has to evaluate the residues at the Matsubara frequencies concerning the contour integration done in the complex energy plane. The Green function has to be determined exactly at these frequencies to simulate the influence of finite temperatures. Effectively, this corresponds to an introduction of the Fermi-Dirac distribution into the electronic structure calculations. A successful method applying this technique is splitting the infinite sum of Matsubara frequencies into a finite sum and a contour integral [21].

For $Fe_{0.72}Cr_{0.18}Ni_{0.1}$ we used a face-centered cubic (fcc) crystal structure with a lattice parameter of 3.59 Å [22], whereas for Fe in the fcc structure (austenite, γ-Fe) we used 3.52 Å [23]. The convergence of the self-consistent potentials have been carefully checked with a number of 834 k points in the irreducible part of the Brillouin zone.

B. Electron heat capacity

The electronic contribution to the specific heat considering a constant volume of a metal can be calculated by taking the partial differential over total electron energy density with respect to the electron temperature $C_e = \partial U/\partial T_e|_V$. The specific heat of the electron gas in dependence on the electronic temperature is described as [24,25]:

$$C_e(T_e) = \int_{-\infty}^{+\infty} (E - E_F) \frac{\partial f(E,\mu,T_e)}{\partial T_e} g(E) \mathrm{d}E, \qquad (3)$$

where $g(E)$ is the DOS at energy E, $f(E,\mu,T_e)$ is the Fermi-Dirac distribution function, E_F is the Fermi energy, and μ the chemical potential. The Fermi distribution, which gives the occupation number of a particular energy level, is defined as:

$$f(E,\mu,T_e) = \frac{1}{e^{(E-\mu)/k_B T_e} + 1}. \qquad (4)$$

The evaluation of the electron heat capacity from Eq. (3) requires the determination of the electronic DOS and the derivative of the Fermi distribution function with respect to the electron temperature. The temperature derivative of Fermi function is only nonzero near E_F. The determination of $\partial f/\partial T_e$ in Eq. (3) at higher temperatures requires the evolution of the chemical potential as a function of the electron temperature $\mu(T_e)$.

The chemical potential can be interpreted as characteristic energy, which defines the internal energy change of the system under conditions of constant entropy and volume, when a particle is added: $\mu = \partial U/\partial N|_{S,V}$ [26,27]. At a temperature of 0 K all states below E_F are filled whereas above E_F all

states are empty. Therefore the system must be in an energetic minimum. The entropy is related to the number of possible microstates. For a system containing a certain number of particles only one exist with an energetic minimum. For this ground state the entropy is equal to zero [28]. After the addition of one particle, the system must be in the ground state of the new system for reaching thermal equilibrium at absolute zero temperature. Thus, by adding one particle above E_F the internal energy enhancement in the system must be equal to E_F and the entropy remains zero [26].

If the electron temperatures are essentially lower than the Fermi temperature, the chemical potential can be approximated by the Sommerfeld expansion for the free electron gas (FEG) model [25]. With the Sommerfeld expansion of the free electronic energy for metals the well-known linear temperature dependence of electron heat capacity can be derived. However, at high electron temperature the Sommerfeld theory of metals is not valid and the electron heat capacity can be calculated for excited electrons from Eq. (3) by using a precise description of the electronic properties of the DOS. The chemical potential $\mu(T_e)$ as a function of the electron temperature can be found directly by evaluating Eq. (5) at various electron temperatures T_e. For the integration the value of the integral must be constant to the value of the electronic density $n_e = N_e/V$ [25]:

$$n_e = \int_{-\infty}^{+\infty} f(E,\mu(T_e),T_e)\cdot g(E)\mathrm{d}E. \tag{5}$$

C. Electron-phonon coupling factor

The first theory of evaluating the electron-phonon coupling factor for metals was done by Kaganov *et al.* [29]. The model is based on the electron-lattice energy exchange rate by consideration of the electron relaxation time. Under the condition that the electron temperature is equal to the lattice temperature, a constant coupling factor can be obtained. In the next step a model was introduced by Chen *et al.*, in which electron-electron and electron-phonon relaxation times are included [30]. The constant value of the electron-phonon coupling factor estimated by Kaganov and the linear temperature dependence proposed by Chen are limited to low electron temperatures and are not valid for high electron temperatures. At high electron temperatures, however, the thermal excitation must be considered. The electrons located below E_F begin to contribute to the electron-phonon energy exchange rate. The free electron gas model cannot be applied and the full spectrum of the electronic DOS for metals is required.

The model for the calculation of the electron-phonon coupling factor is based on a general description of the electron-phonon energy exchange rate with two distinct temperatures developed by Allen [31]. Wang *et al.* extended this theoretical model by inclusion of d-band states for thermal excitation at higher electron temperatures in order to get accurate results for Au in comparison with time-resolved electron temperature measurements [32]. In his work Lin *et al.* [6] has rewritten the theory corresponding to the electron-phonon coupling factor by merging the theory of Allen and Wang to compare it with the free electron gas model of various transition metals. The temperature dependence of electron-phonon coupling factor within this approach can be expressed as

$$G(T_e) = \frac{\pi\hbar k_B \lambda\langle\omega^2\rangle}{g(E_F)}\int_{-\infty}^{+\infty} g^2(E)\left(-\frac{\partial f}{\partial E}\right)\mathrm{d}E, \tag{6}$$

where λ is the dimensionless electron-phonon mass enhancement parameter [33] and $\langle\omega^2\rangle$ is the second moment of the phonon spectrum defined by McMillan [34], and $g(E_F)$ is the electron DOS at the Fermi level E_F. At low electron temperature $-\partial f/\partial E$ reduces to a delta function centered at E_F and Eq. (6) yields a constant value for the electron-phonon coupling factor. Whereas at high electron temperatures the delta function at energy E is shifting away from E_F. This shift of E_F causes a temperature dependence of the electron-phonon coupling factor. The material parameter $\lambda\langle\omega^2\rangle$ can be obtained by using the calculated or experimental value of λ [35] and the approximation $\langle\omega^2\rangle = \theta_D^2/2$ [36].

Sacchetti proposed a simple model for treating the electron-phonon interaction in binary alloys by applying the CPA to calculate the specific heat enhancement. Within this approximation in random binary alloys a description for electron-phonon enhancement factor is developed. It is given by the average of the local enhancement factors considering a weak-scattering system $\lambda = x\lambda_A + y\lambda_B$ [37].

In the absence of λ for ternary Fe alloys a quantitative estimation we extended Sacchetti's approximate description to three components

$$\lambda = x\lambda_A + y\lambda_B + z\lambda_C, \tag{7}$$

whereby λ_A, λ_B, and λ_C are separated electron-phonon enhanced effective electron masses of alloy compounds denoted with A, B, and C, and its composition fraction x, y, and z, respectively.

III. RESULTS

A. Ground state properties of γ-Fe and $Fe_{0.72}Cr_{0.18}Ni_{0.1}$

The ground state properties of γ-Fe and $Fe_{0.72}Cr_{0.18}Ni_{0.1}$ are the basis of the additional calculations for the thermal properties. In Figs. 1(a) and 1(b) the Bloch spectral functions of bulk γ-Fe and $Fe_{0.72}Cr_{0.18}Ni_{0.1}$ are shown. The Bloch spectral function can be interpreted as k-resolved DOS in reciprocal space. There are mainly two types of bands visible. For the energy range from -10 eV to -5 eV an s band dominates the k path from X to Γ. Around E_F detailed bands occur migrating from the d states of γ-Fe. These bands essentially define the electronic and magnetic properties of γ-Fe and $Fe_{0.72}Cr_{0.18}Ni_{0.1}$.

For $Fe_{0.72}Cr_{0.18}Ni_{0.1}$ a broadening of the d bands applies whereas the s band is unaffected. The broadening of electronic bands due to chemical and magnetic disorder is a well known effect that has been investigated in previous works [38,39]. This has an impact on the magnetic and electronic properties as well as the thermal properties important for the laser ablation.

B. Thermal properties of Fe and $Fe_{0.72}Cr_{0.18}Ni_{0.1}$

In the following, the calculations for the DOS as well as for the thermal properties of $Fe_{0.72}Cr_{0.18}Ni_{0.1}$ are presented. The electronic structure calculations of the ground state are

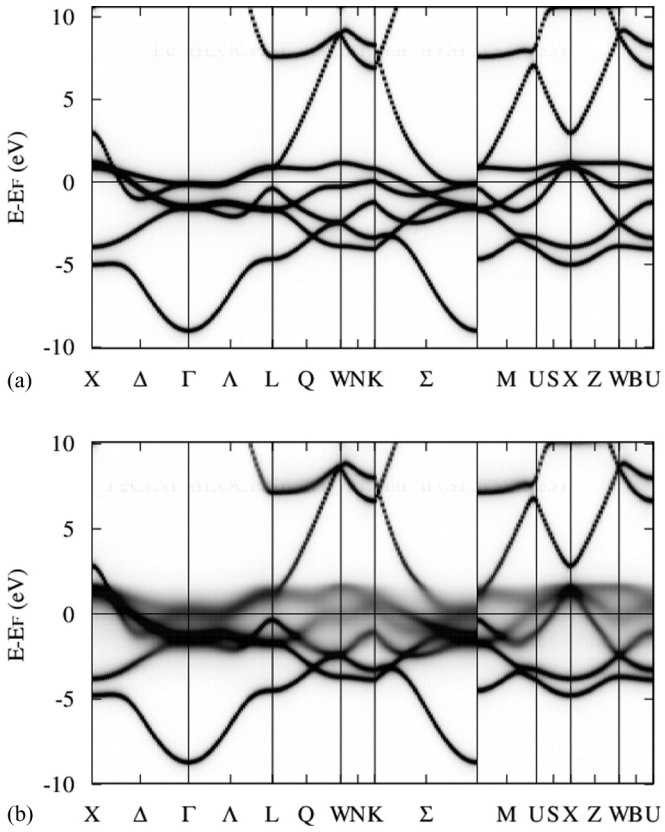

FIG. 1. (a) Bloch spectral function of γ-Fe, (b) Bloch spectral function of $Fe_{0.72}Cr_{0.18}Ni_{0.1}$. The calculations of the band structure are performed by using the SPR-KKR program package [10]. The energy is denoted with respect to Fermi energy E_F.

performed with the SPR-KKR package for a realistic description of the paramagnetic properties. The electron heat capacity and the electron-phonon coupling factor were compared between γ-Fe and $Fe_{0.72}Cr_{0.18}Ni_{0.1}$. A similar electronic DOS for Fe bulk with the fcc structure was calculated by Lin *et al.* using the Vienna *ab initio* simulation package (VASP). Thus, based on this electron DOS from Lin *et al.* comparable thermal properties of Fe were calculated [40]. In Fig. 2(a) the electronic DOS for $Fe_{0.72}Cr_{0.18}Ni_{0.1}$ (fcc) and γ-Fe (fcc) indicate similar characteristics of the electronic DOS. In the range of -9eV and -5 eV for $Fe_{0.72}Cr_{0.18}Ni_{0.1}$ and γ-Fe an s band can be identified. A major common feature is the presence of a high DOS in the range between -5 eV and 2 eV. This region can be associated with the occurrence of a d band. In the case of $Fe_{0.72}Cr_{0.18}Ni_{0.1}$ the d band reaches $\sim$2 eV above Fermi energy level and thus is not occupied. However, the d-band edge of Fe is located $\sim$1 eV closer to E_F. At energies -1 eV and -2 eV below E_F a distinct characteristic peak of the electronic DOS of $Fe_{0.72}Cr_{0.18}Ni_{0.1}$ vanishes in comparison to Fe. As a result the d band of γ-Fe has a higher occupation number compared to $Fe_{0.72}Cr_{0.18}Ni_{0.1}$. With that a larger number of electrons can be excited into the conduction band affecting the electronic heat capacity C_e and the electron-phonon coupling factor G.

The predicted temperature dependence of the chemical potential for γ-Fe and $Fe_{0.72}Cr_{0.18}Ni_{0.1}$ is shown in Fig. 2(b). At low electron temperature $\sim 10^3$ K with respect to the energy $\sim$0.1 eV the thermal excitation of the s band is the dominant effect. The chemical potential remains nearly constant because the internal energy change is equal to E_F and the entropy remains zero. At higher electron temperatures, however, the electrons at the energy levels below E_F can easily be excited. The electronic excitation to the conduction band leads to a shift of the chemical potential to higher energies [Fig. 2(b)]. The excitation of electrons change the number of occupied states below and above E_F. As a result the chemical potential must shift to higher energies to keep constant the total number of electrons. The shift of the chemical potential is a consequence of the change in the electronic occupation by thermal excitation. Because of that the fundamental distinction of the chemical potential for $Fe_{0.72}Cr_{0.18}Ni_{0.1}$ and γ-Fe can be reduced to a different d-band structure around E_F and in following the number of accessible excited states.

Figure 2(c) shows the temperature dependence of the electron heat capacity. The electron heat capacity of γ-Fe and of $Fe_{0.72}Cr_{0.18}Ni_{0.1}$ was calculated by inserting the results for the chemical potential and the DOS of γ-Fe and $Fe_{0.72}Cr_{0.18}Ni_{0.1}$ into Eq. (3). For electron temperatures $\sim 5 \times 10^4$ K the electron heat capacity of γ-Fe and $Fe_{0.72}Cr_{0.18}Ni_{0.1}$ follows almost a linear behavior up to a local peak at $\sim 1 \times 10^4$ K. The predicted linear dependence is affected by excitations from the occupied states of the d band close to E_F. The calculated slope of the linear temperature dependence for the γ-Fe amounts to 650 $J/m^3/K^2$, corresponding to 4.3 $J/mol/K^2$. This value is in good agreement with the reported data of $\sim$4 $J/mol/K^2$ and 4.5 $J/mol/K^2$ for γ-Fe in the fcc structure [41,42]. Indeed, the lower number of exited electrons from the d band around the Fermi energy of $Fe_{0.72}Cr_{0.18}Ni_{0.1}$ results in a lower slope in the linear part of the electronic heat capacity with the amount of 580 $J/m^3/K^2$, corresponding to 4 $J/mol/K^2$. The number of excited electrons are determined by the width of thermal excitation ($\sim k_B \cdot T_e$) in an energy interval around E_F and the increase of the number of conductive electrons in the s band. With an increase of the electron temperature above $\sim 5 \times 10^3$ K the chemical potential shift to higher energies. This creates a slightly drop of the curve till a minimum with a subsequent increase of heat capacity above electron temperature $\sim 2.4 \times 10^4$ K. At higher electron temperatures a deviation of the electron heat capacity about 5% comparing γ-Fe and $Fe_{0.72}Cr_{0.18}Ni_{0.1}$ occurs [Fig. 2(c)]. This results from the shift of the chemical potential to the d-band edge. The number of possible states of Fe located at $\sim$1 eV and $\sim$0.5 eV above E_F can contribute directly to the electron heat capacity by thermal excitation. This exhibits a decline in the electron heat capacity of $Fe_{0.72}Cr_{0.18}Ni_{0.1}$ at high electron temperatures. With that a low deviance of stored electron heat with respect to the change of the electron temperature is revealed between γ-Fe and $Fe_{0.72}Cr_{0.18}Ni_{0.1}$. Thus, the predicted trend of the electron heat capacity C_e causes a similar transient evolution of the electron temperature in the electron subsystem of γ-Fe and $Fe_{0.72}Cr_{0.18}Ni_{0.1}$ during the time of the electron-lattice nonequilibrium processes induced in a metal target by the fast laser energy deposition with ultrashort laser pulses.

The electron heat capacity is also sensitive to the electronic structure calculation of the DOS discussed above in either instance for $Fe_{0.72}Cr_{0.18}Ni_{0.1}$ and γ-Fe. The excitation of d-band electrons has a strong effect for the temperature dependence of the electron heat capacity and must be taken into account in the estimation of the electron-phonon coupling.

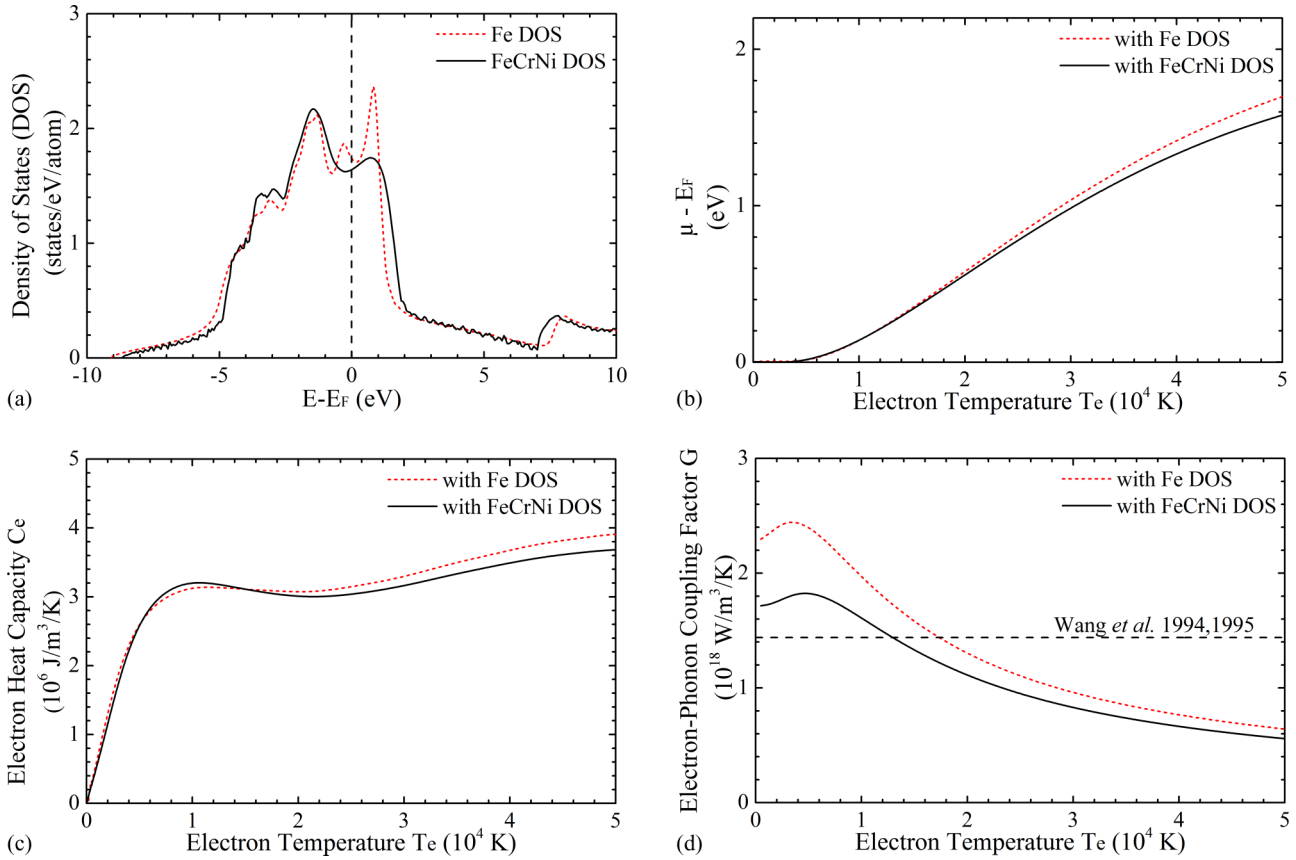

FIG. 2. (a) The electron DOS calculation for $Fe_{0.72}Cr_{0.18}Ni_{0.1}$ obtained at a temperature of 0 K. The energy is denoted with respect to the Fermi energy E_F.(b) The chemical potential μ as a function of the electron temperatures, (c) the electron heat capacity C_e, (d) the electron-phonon coupling factor G as a function of the electron temperature using the material parameter $\lambda\langle\omega^2\rangle = 217.75$ meV^2 for γ-Fe and $\lambda\langle\omega^2\rangle = 183.44$ meV^2 for $Fe_{0.72}Cr_{0.18}Ni_{0.1}$.

The calculation of the electron temperature dependence of the electron-phonon coupling is performed with Eq. (6), which requires the information of $\lambda\langle\omega^2\rangle$. The value for $Fe_{0.72}Cr_{0.18}Ni_{0.1}$,$\lambda\langle\omega^2\rangle = 183.44$ meV^2, is estimated by approximation from Eq. (7) and $\langle\omega^2\rangle = \theta_D^2/2$ using an experimental value of the Debye temperature $\theta_D = 468$ K for AISI 304 at T = 0 K [43]. In Table I the values of λ calculated by self-consistent band structure methods and the measured Debye temperatures for Fe, Cr, Ni are listed.

The electron temperature dependence of the electron-phonon coupling factor $G(T_e)$ predicted for γ-Fe and $Fe_{0.72}Cr_{0.18}Ni_{0.1}$ is very similar and exhibits the same qualitative features as shown in Fig. 2(d). The features of both dependencies are an increase of the electron-phonon coupling factor up to $\sim 4 \times 10^3$ K, followed by a decrease with further temperature rise. The rise of the electron-phonon coupling factor at electron temperatures below $\sim 4 \times 10^3$ K can be explained by thermal excitations of a large number of d-band electrons, which contribute to the electron-phonon collision and accordingly to energy exchange. The increase of the electron-phonon coupling factor indicates a faster energy transfer by the electron-phonon scattering process from hot electrons to the lattice within the framework of TTM.

TABLE I. The material parameter $\lambda\langle\omega^2\rangle$ estimated by using the calculated value of λ [36] and the suggested approximation $\langle\omega^2\rangle = \theta_D^2/2$ meV^2. λ is the dimensionless electron-phonon mass enhancement parameter and θ_D is the Debye temperature (K) for Fe,Cr,Ni taken from Papaconstantopoulos *et al.* [36]. The Debye temperature for FeCrNi is used from Ledbetter *et al.* [43].

	Fe	Cr	Ni	FeCrNi
λ	0.270	0.131	0.084	0.226
θ_D	467	630	450	468
$\lambda\langle\omega^2\rangle$	217.75	192.27	62.90	183.44

In this paper, the start value of electron-phonon coupling G for $Fe_{0.72}Cr_{0.18}Ni_{0.1}$ at low electron temperatures is reduced to $\sim 1.7 \times 10^{18}$ W/m^3/K. A possible reason can be a lower value of λ at similar values of $\langle\omega^2\rangle$. This decrease of the electron-phonon interaction leads to a lower collision frequency and therefore to smaller energy exchange between electron and lattice at lower electron temperatures. At higher temperatures above 5×10^3 K the excitation of d-band electrons exceeds the high density of the d-band edge of Fe located at 1 eV [Fig. 2(a)]. This shift reduces the contribution of the d-band electrons to the electron-phonon coupling and leads to a rapid drop of the energy exchange rate for γ-Fe. In contrast for $Fe_{0.72}Cr_{0.18}Ni_{0.1}$ the d-band edge is located at an energy of $\sim$2 eV. This leads to a smoother decrease of the electron phonon coupling. With a further electron temperature increase up to $\sim 5 \times$

10^4 K a slower decrease of the electron-phonon coupling can be seen. The predicted temperature dependencies can be interpreted as equilibrium of the excited electrons coming from deeper energies of the d band and continuing shift of the chemical potential to higher energies towards the d-band edge.

The calculated initial value of the electron-phonon coupling factor for Fe at room temperature, shown by the red dashed line in Fig. 2(d) (2.3×10^{18} W/m^3/K) is higher than the independent experimental estimation at 300 K from Wang *et al.* [44] obtained from a previous swift-heavy-ion irradiation experiment (1.44×10^{18} W/m^3/K), in Fig. 2(d) plotted as black dashed line. The value of the electron-phonon coupling factor (1.44×10^{18} W/m^3/K) was estimated from comparison of molten phase radius around the ion path in dependence on electronic energy loss between calculated and experimental latent track radii irradiated by swift heavy ions within the thermal-spike model. This value is by a factor of 1.6 smaller compared to our prediction. In his work Wang *et al.* assumed an uncertainty of 30% resulting from the input parameters and the approximation of the electronic heat capacity and thermal conductivity within the free electron gas theory for the calculation of the molten track radii. The determination of the electron-phonon coupling constant can only be considered as a rough estimation due to these discrepancies [44].

Here, the electron-phonon coupling factor was calculated for a wide electron temperature range assuming a strong electron-phonon nonequilibrium. In contrast, the reported value of the electron-phonon coupling factor was estimated by the calculation of molten track radii. In this respect, the value of the electron-phonon coupling factor (1.44×10^{18} W/m^3/K) can be considered as an "effective" electron-phonon coupling constant and therefore be in a reasonable agreement with our calculations for Fe.

For the analysis of a laser energy deposition in a metal alloy a temporal change of the thermophysical properties of $Fe_{0.72}Cr_{0.18}Ni_{0.1}$ in comparison to γ-Fe during the time of electron-phonon equilibration can appear. Considering $Fe_{0.72}Cr_{0.18}Ni_{0.1}$ a decrease of the electron-phonon coupling strength in a TTM simulation leads to a reduced energy transfer from hot electrons to the lattice. Consequently, a lower transient evolution of the lattice temperature after irradiating with ultrashort laser pulses could lead to an increase of the threshold fluence for the surface melting or laser ablation for $Fe_{0.72}Cr_{0.18}Ni_{0.1}$.

C. Temperature dependent electronic DOS and its influence on $C_e(T_e)$ and $G(T_e)$ in the paramagnetic state of FeCrNi alloy

In the section above the electron heat capacity and the electron-phonon coupling based on the ground state electron DOS at 0 K are presented. The calculation of the paramagnetic ground state DOS of $Fe_{0.72}Cr_{0.18}Ni_{0.1}$ was performed in the framework of the disordered local moment (DLM) approach. According to Gyorffy *et al.* [16] the DLM approach allows the existence of a magnetic polarization with independent spin fluctuations of the local moments, whereby the total magnetization in the paramagnetic state is zero. Considering the austenitic $Fe_{0.72}Cr_{0.18}Ni_{0.1}$ steel alloy in the fcc crystallographic structure of γ-Fe at the higher temperature the paramagnetic phase can be described using an extended method.

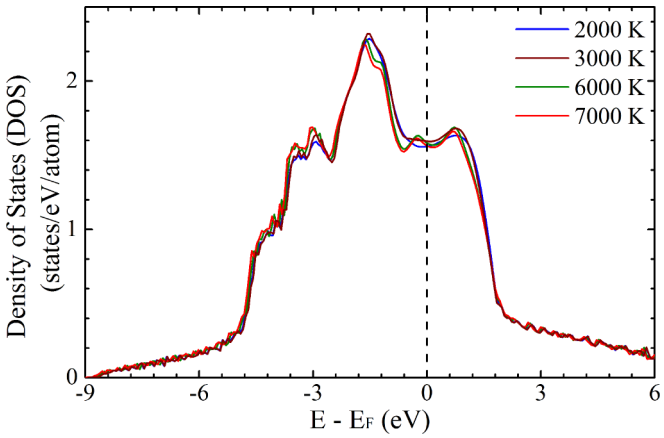

FIG. 3. The total electronic DOS of FeCrNi alloy in dependence on temperature. The computational calculation is performed by using the Matsubara technique at various temperatures. The energy is denoted with respect to E_F.

Therefore the DLM model was used connected with the Matsubara technique for a self-consistent treatment of the considered alloy system at higher electron temperature. In that framework the paramagnetic state provided by the DLM model is described considering a change in the electronic temperature. As a result of these calculations the DOS for $Fe_{0.72}Cr_{0.18}Ni_{0.1}$ at different electron temperatures is shown in Fig. 3.

According to the Matsubara technique the calculations was done considering finite temperatures including the Fermi-Dirac distribution in our Green function approach [21]. The calculations are numerical stable up to ~7000 K. However, only small changes of the fine structure occur going to higher electron temperatures. These changes affect the electron heat capacity and the electron-phonon coupling factor only slightly. According to the magnetic properties our calculations induce a decrease of the disordered local magnetic moment of Fe going to higher electron temperatures as one would expect. At an electron temperature ~4000 K the local spin and orbital magnetic moment are almost zero.

In Fig. 4(a) the total electronic DOS is shown as calculated via DLM and by considering an electron temperature of 7000 K. A convergence between both DOS is clearly recognizable, whereby only at ~1 eV and below at −3 eV small differences are visible. This affects the electronic heat capacity as it shifts the minimum from $\sim 2 \times 10^4$ K to lower values [Fig. 4(c)]. This shift in the electron temperature is caused by a reoccupation of the d band above E_F. Going to higher electron temperatures the electronic heat capacity raises as proposed by the DLM model. The energy transfer from the electronic subsystem to the lattice in Fig. 4(d) shows a deviation of ~5% concerning previous calculation especially at lower electron temperature. In this temperature region the electron-phonon coupling factor increases until a local maximum at ~4000 K. For higher electron temperatures the electron-phonon coupling factor as calculated for ~7000 K converges to the result at 0 K. Accordingly, the deviation between the the temperature dependent electronic DOS [Fig. 4(a)] and the DOS of the pure DLM model [Fig. 2(a)] are weak in the case of electron-phonon coupling strength, especially at higher electron temperature.

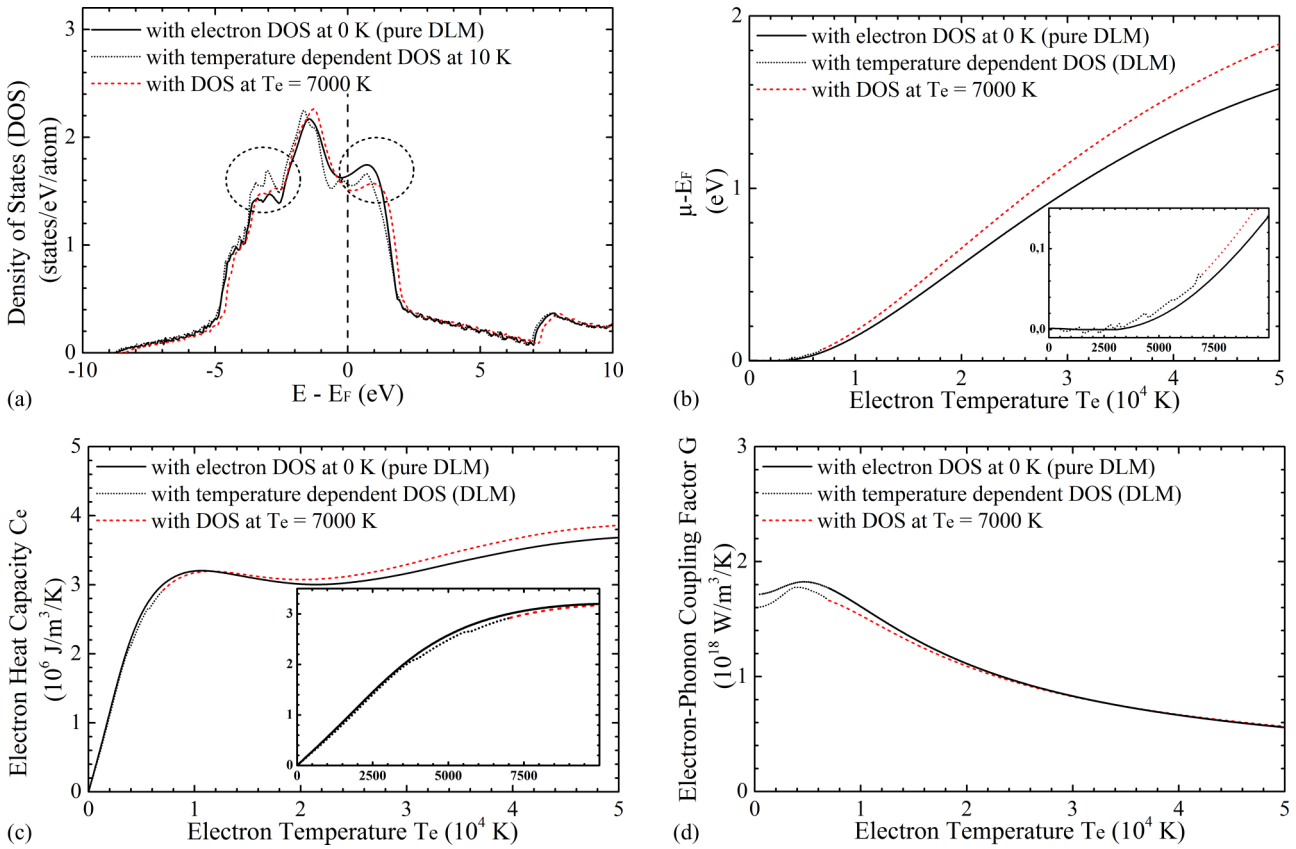

FIG. 4. (a) The electron DOS calculation for $Fe_{0.72}Cr_{0.18}Ni_{0.1}$ is calculated at different temperatures using the Matsubara technique. The energy is denoted with respect to E_F, (b) the chemical potential μ as a function of the electron temperatures, (c) the electron heat capacity C_e, (d) the electron-phonon coupling factor G.

At a material irradiation with ultrashort laser pulse the electron temperature can reach several thousand Kelvins within the electron-lattice nonequilibrium process during the first tens of picoseconds, whereby electron temperature of $\sim 10^4$ K is quickly exceeded. In this respect, a deviation of $\sim$5% in the computing of the electron-phonon strength in a range of temperatures accessible in the laser material processing does not play a significant role for electron-lattice energy exchange.

IV. SUMMARY

In this paper, calculation of the electron heat capacity and the electron-phonon coupling factor dependence on the electron temperature for the stainless steel alloy $Fe_{0.72}Cr_{0.18}Ni_{0.1}$ (AISI 304) is presented. The calculation of electronic thermophysical parameters are based on detailed analysis of the electronic DOS obtained from the Munich SPR-KKR band structure program. With that we determined the properties of the electronic distribution for a randomly disordered system modeling $Fe_{0.72}Cr_{0.18}Ni_{0.1}$. Additionally, the influence on electron heat capacity and electron-phonon coupling factor of $Fe_{0.72}Cr_{0.18}Ni_{0.1}$ in the paramagnetic phase at higher electron temperatures was investigated using the DLM model connected with the Matsubara technique.

The electron heat capacity and the electron-phonon coupling factor of $Fe_{0.72}Cr_{0.18}Ni_{0.1}$ show an increase affected by the thermal excitation in a wide range of the d band with a high DOS at electron temperatures below 5×10^3 K. By exceeding 10^4 K a nonequilibrium of the excited d-band electrons and a reoccupation induced by shifting of the chemical potential to higher energies leads to a strong decrease of the electron-phonon coupling, whereas the electron heat capacity remains at considerably constant high values. The comparison with γ-Fe indicates a similar qualitative and quantitative trend of the electron heat capacity of $Fe_{0.72}Cr_{0.18}Ni_{0.1}$ attributable to the high Fe content of 72 % in the alloy. The negative deviation of electron-phonon coupling between $Fe_{0.72}Cr_{0.18}Ni_{0.1}$ and γ-Fe by $\sim$25% is due to electron-phonon interaction.

Overall, a good agreement between the calculation of the electron heat capacity and the electron-phonon coupling factor of $Fe_{0.72}Cr_{0.18}Ni_{0.1}$ and γ-Fe was observed. The calculation of the thermal properties in the paramagnetic state of the austenitic $Fe_{0.72}Cr_{0.18}Ni_{0.1}$ with temperature dependent electronic DOS shows a weak difference of the electron heat capacity and the electron-phonon coupling strength compared to $Fe_{0.72}Cr_{0.18}Ni_{0.1}$ at the ground state.

Finally, the calculation of the electron-phonon coupling strength for the $Fe_{0.72}Cr_{0.18}Ni_{0.1}$ alloy is based on the literature values of the electron-phonon mass enhancement factor λ. Here, the empirical data of λ and the experimental electron-phonon coupling constant at room temperatures are weak for alloy materials. Further measurements of the electron-phonon coupling with time-resolved experiments or thermomodula-

tion experiments are necessary to obtain a better understanding of the differences between pure metals and their related alloys.

ACKNOWLEDGMENTS

The authors gratefully acknowledge the financial support by the Deutsche Forschungsgemeinschaft (HU1893/2-1). This work was also partly funded by the Seventh Framework Programme (310220), CENTEM PLUS (LO1402) and the Munich School of Engineering within the framework of the TUM Applied Technology Forum. Additionally, we would like to thank Prof. J. Staunton from Department of Physics in University of Warwick, Coventry, for discussions concerning DLM and energy path including Matsubara technique.

[1] I. M. Burakov, N. M. Bulgakova, R. Stoian, A. Rosenfeld, and I. V. Hertel, Appl. Phys. A **81**, 1639 (2005).
[2] D. Bäuerle, R. Denk, J. D. Pedarnig, K. Piglmayer, J. Heitz, and G. Schrems, Appl. Phy. A **77**, 203 (2003).
[3] W. Hu, Y. C. Shin, and G. B. King, J. Manuf. Sci. Eng. **132**, 011009 (2010).
[4] S. I. Anisimov, B. L. Kapeliovich, and T. L. Perelman, Sov. Phys. JETP **39**, 375 (1974).
[5] S. I. Anisimov and B. Rethfeld, Proc. SPIE **3093**, 192 (1997).
[6] Z. Lin, L. V. Zhigilei, and V. Celli, Phys. Rev. B **77**, 075133 (2008).
[7] G. V. Raynor, Rep. Prog. Phys. **15**, 173 (1952).
[8] Z. Lin and L. V. Zhigilei, Proc. SPIE **6261**, 62610U (2006).
[9] Z. Lin and L. V. Zhigilei, Appl. Surf. Sci. **253**, 6295 (2007).
[10] H. Ebert *et al.*, *The Munich SPR-KKR package*, version 6.3, http://olymp.cup.uni-muenchen.de/ak/ebert/SPRKKR, 2012.
[11] J. Korringa, Physica **13**, 392 (1947).
[12] W. Kohn and N. Rostoker, Phys. Rev. **94**, 1111 (1954).
[13] H. Ebert, K. Ködderitzsch, and M. J., Rep. Prog. Phys. **74**, 096501 (2011).
[14] B. Velický, S. Kirkpatrick, and H. Ehrenreich, Phys. Rev. **175**, 747 (1968).
[15] S. S. A. Razee and R. Prasad, Phys. Rev. B **45**, 3265 (1992).
[16] B. L. Gyorffy, A. J. Pindor, J. B. Stauton, G. M. Stocks, and H. Winter, J. Phys. F **15**, 1337 (1985).
[17] L. Vitos, P. A. Korzhavyi, and B. Johansson, Nat. Mater. **2**, 25 (2003).
[18] R. Mills, L. J. Gray, and T. Kaplan, Phys. Rev. B **27**, 3252 (1983).
[19] B. Ginatempo and J. B. Staunton, J. Phys. F: Metal Physics **18**, 1827 (1988).
[20] S. Vosko, L. Wilk, and M. Nusair, Can. J. Phys. **58**, 1200 (1980).
[21] K. Wildberger, P. Lang, R. Zeller, and P. H. Dederichs, Phys. Rev. B **52**, 11502 (1995).
[22] F. C. Nascimentob and C. M. Lepienskia, Mater. Res. **12**, 173 (2009).
[23] R. Shashanka and D. Chaira, Mater Charact **99**, 220 (2015).
[24] C. Kittel, *Introduction to Solid State Physics*, 7th ed. (Wiley, New York, 1996).
[25] N. W. Ashcroft and N. D. Mermin, *Solid State Physics* (Harcourt College Publishers, Orlando, 1976).
[26] R. Baierlein, Am. J. Phys. **69**, 423 (2001).
[27] G. Cook and R. H. Dickerson, Am. J. Phys. **63**, 737 (1995).
[28] J. Wilks, *The Third Law of Thermodynamics*, repr ed., Oxford library of the physical sciences (Univ. Press, Oxford, 1972).
[29] M. I. Kaganov, I. M. Lifshitz, and L. V. Tanatarov, Sov. Phys. JETP **4**, 173 (1957).
[30] J. K. Chen, W. P. Latham, and J. E. Beraun, J. Laser Appl. **17**, 63 (2005).
[31] P. Allen, Phys. Rev. Let. **59**, 1460 (1987).
[32] X. Y. Wang, D. M. Riffe, Y.-S. Lee, and M. C. Downer, Phys. Rev. B **50**, 8016 (1994).
[33] G. Grimvall, Phys. Scr. **14**, 63 (1976).
[34] W. L. McMillan, Phys. Rev. **167**, 331 (1968).
[35] S. Y. Savrasov and D. Y. Savrasov, Phys. Rev. B **54**, 16487 (1996).
[36] D. A. Papaconstantopoulos, L. L. Boyer, B. M. Klein, A. R. Williams, V. L. Morruzzi, and J. F. Janak, Phys. Rev. B **15**, 4221 (1977).
[37] F. Sacchetti, J. Phys. F **10**, 801 (1980).
[38] K. W. Lee and W. E. Pickett, Phys. Rev. B **73**, 075105 (2006).
[39] R. M. Martin, *Electronic Structure: Basic Theory and Practical Methods* (Cambridge University Press, Cambridge, 2004).
[40] Electronic thermophysical properties of transition metals are accessible in tabulated form at http://www.faculty.virginia.edu/compmat/electronphonon-coupling.
[41] E. Wasserman, L. Stixrude, and R. E. Cohen, Phys. Rev. B **53**, 8296 (1996).
[42] D. A. Boness, J. Brown, and A. McMahan, Physics of the Earth and Planetary Interiors **42**, 227 (1986).
[43] H. M. Ledbetter, W. F. Weston, and E. R. Naimon, J. Appl. Phys. **46**, 3855 (1975).
[44] Z. G. Wang, C. Dufour, E. Paumiert, and M. Toulemonde, J. Phys.: Condens. Matter **7**, 2525 (1994).